

Valving in Microchannels via Electrodeposition on Solid Electrolytes

M. N. Kozicki, P. Maroufkhani, and M. Mitkova

Center for Solid State Electronics Research, Arizona State University, Tempe, AZ 85287, USA

ABSTRACT

Microfluidic technology is currently being applied to analytical systems but suitable valving elements are proving to be difficult to implement. We have recently developed a novel way to electrically regulate flow through microchannels via a structure that can be made using readily available microfabrication techniques. An electrical signal is used to stimulate silver deposition on a thin Ag-Ge-Se solid electrolyte layer in a small region of a channel. The electrodeposited silver, which is a high surface area fractal structure less than 1 μm in height and several hundred μm long, changes the fluid-surface interaction. In this paper we demonstrate that this effect can be used to regulate pressure-driven flow in a microchannel.

Keywords: microfluidics, valve, solid electrolyte, chalcogenide, electrodeposition.

1 INTRODUCTION

Miniaturization of analytical processes has become a significant area of research and development in the past decade. Factors driving the development of microanalytical devices include the need for a reduction in analyte consumption, the ability to work with extremely small sample volumes, decrease in analysis time, and overall reduction in system/operational costs [1]. Leading-edge microanalytical devices are typically fabricated using techniques and materials borrowed largely from the microelectronics industry. The ultimate objective is the integration of multi-step and complex analytical procedures, such as metering and mixing of reagents, thermal cycling, labeling and fragment analysis, into a single “lab-on-a-chip”. Integration and development of microfluidic technology requires control of fluid flow within the microsystem. However, batch production of microfluidic systems demands development of integrated fluid handling schemes that are not only reliable and cost effective but also allow the use of standard (and therefore widely available) microfabrication techniques and on-chip control systems. Various valves with a variety of actuation methods have been devised and prototyped but most current approaches are expensive, unreliable, or power-hungry as they utilize micromachined mechanical moving parts or thermal actuation.

We have recently developed a novel way to electrically regulate flow through microchannels via a structure that can be made using common microfabrication techniques. We use an electrical signal to stimulate silver deposition on a

thin Ag-Ge-Se solid electrolyte layer in a small region of a microchannel. The electrodeposit can extend for several hundred microns if the electrolyte is fed with silver from the anode, the ions in the electrolyte being reduced by electrons from the cathode. The electrodeposited silver, which is a high surface area fractal structure less than 1 μm in height, changes the fluid-surface interaction, increasing the contact angle for water by at least 20° over that measured on solid electrolyte alone [2]. Since fluid flow in a microchannel is dominated by the nature of the channel surface, this increase in effective hydrophobicity can be used to control the movement of the fluid.

In this paper we show the initial results from the use of this technique in a microfluidic testbed. The testbed’s 200 μm wide channel has a depth of 18 μm and yet a sub-micron (in height) electrodeposit grown across the channel floor is able to completely halt pressure-driven liquid flow.

2 MATERIAL SYSTEM

Many materials can conduct ions but it is the Ag-Ge-Se ternaries that are of particular interest to us in microfluidic applications as they exhibit high ion mobility at normal device operating temperatures and are easy to form as thin films on devices. An example of a ternary electrolyte that we have studied extensively is $\text{Ag}_{0.33}\text{Ge}_{0.20}\text{Se}_{0.47}$ [3], which is essentially a glassy Ge-rich backbone mixed with a *superionic* Ag_2Se phase. The distinctive nanostructure of this material leads to a stable solid electrolyte that operates over a wide range of temperature. In addition, electrodeposit growth rate is high with this particular composition and the electrodeposited silver features tend to be continuous with a high fractal dimension [4]. This electrodeposit morphology is ideal for our microvalve application. We typically form the ternary electrolyte in a two step process in which a binary ($\text{Ge}_{0.30}\text{Se}_{0.70}$) base glass is deposited first and then capped with a thin silver film, the two layers being combined by *photodissolution* using ultraviolet light. The relative thicknesses of these layers are chosen to allow complete saturation of the base glass with the silver, which occurs when the silver combines with all the Se atoms available for reaction.

In solid electrolytes, only the positively charged ions are able to move and the negative charge centers are fixed. Electrodeposition, which results in a net decrease in ion concentration at the cathode, will only proceed if there is a net supply of metal ions into the electrolyte from an oxidizable silver anode. Of course, the mass of silver at the anode must be at least as great as the mass to be electrodeposited. Electrodeposition also requires an applied

bias above a particular threshold to overcome the effects of the cathodic barrier. The intrinsic potential difference necessary to do this is typically only a few hundred mV but long structures that have a high series resistance will require higher voltages to initiate electrodeposition as most of the applied voltage will be dropped across the electrolyte.

The ions nearest the electron-supplying cathode will be reduced first and statistical non-uniformities in the ion concentration and in the topography of the electrode will tend to promote localized deposition or nucleation rather than blanket plating. For a wide electrode (e.g., several hundred μm), only a few nuclei will be favored for subsequent growth, extending out from the cathode. Note that the electrodeposition of metal on the cathode does not mean that ions entering from the oxidizable anode have to travel the entire length of the structure to replace those that are reduced. The ion closest to the reduced ion will move to the vacated negative site on the hosting material and those upstream will do likewise, each filling the vacated site of the one downstream, until the last vacated space closest to the anode is filled by the incoming ion, an effect known as a *coordinated motion*. Since the electrodeposit is physically connected to the cathode, it can supply electrons for subsequent ion reduction so the growing electrodeposit will harvest ions from the electrolyte, plating them onto its surface to extend itself outwards from the cathode. This leads to growth of electrodeposits that can be several hundred microns in length on the surface of the electrolyte. Note that by Faraday's Law, the amount of material electrodeposited equals the amount of charge supplied by the external circuit so growth rate will tend to be limited by how much electron current can be made to flow in the electrolyte. This typically means that since the overall electrolyte series resistance can easily be in the $\text{G}\Omega$ range, several volts may be required to produce reasonable growth rates.

3 TEST STRUCTURE FABRICATION

To demonstrate how surface electrodeposition on solid electrolytes could be used in a valving scheme, we created a microfluidic "testbed". The fabrication process begins with a cleaned (100) silicon substrate covered with 2000 \AA of wet-grown oxide which will act as a surface mask during the channel etch process. A 1 μm thick layer of OCG 825 positive photoresist is spun onto the sample and a soft bake performed at 80 $^{\circ}\text{C}$ for 30 minutes to drive off the solvents in the resist. Following this, the channel regions are defined using a dark field mask and a Karl Suss MJB-3 contact printer/aligner, exposing for 20 s at 3.8 mW/cm^2 . The pattern is then developed using OCG 945 developer for 45 s and the sample is hard baked for 60 minutes at 120 $^{\circ}\text{C}$. Finally, to pattern the oxide, the wafer is etched in 10:1 hydrofluoric acid:DI water for 10 minutes and the photoresist removed using Microstrip 2001 photoresist stripper at 75 $^{\circ}\text{C}$ for 25 minutes. The etched windows in the

oxide form a pattern which has a 0.2 mm x 10 mm channel region with 3 mm x 3 mm reservoirs at either end. The actual channels are etched into the underlying silicon substrate using 30 wt.% KOH solution and 2 vol.% isopropanol, the latter decreasing the surface tension of the solution to promote smooth etching. The etching process is performed at 80 $^{\circ}\text{C}$ for 15 minutes with continuous stirring and results in 18 μm deep microchannels in the silicon. The sample is then immersed in HF for 10 minutes to remove the remaining silicon dioxide surface mask. Since KOH is an anisotropic etchant, the channels produced have a trapezoidal cross-section with sloped sidewalls. This is actually advantageous in the context of our devices as it aids the step coverage of the electrolyte layer.

The solid electrolyte is now formed on the sample. Great care must be taken while depositing chalcogenide glasses because the elements evaporate at different rates due to the difference in their partial vapor pressures. For the case of $\text{Ge}_x\text{Se}_{1-x}$, the selenium has a higher vapor pressure than germanium, therefore, it will evaporate faster and with higher energy and this will have a great impact on the composition of the deposited film. Thus, in order to control the evaporation rate of the compounds in the chalcogenide glass and maintain the composition of the deposited film so that it is close to that of the source material, a specially designed semi-Knudsen cell evaporation boat is used. This boat consists of a stainless steel rectangular frame on which a tungsten foil is wound to act as a diffuser. The openings in the diffuser are larger than the orifices of a typical Knudsen cell so that the deposition rate is reasonably high but small enough so as not to disturb the equilibrium vapor pressure inside the boat. Once the chalcogen vapor strikes this cover, part will go through after losing a considerable amount of energy, and the remainder re-fills the semi-Knudsen cell. After the entire volume of the cell is filled with chalcogen vapor, the vapor exerts pressure over the source and prevents it from further emitting this material. At this point, the second element (germanium) starts to evaporate when the pressure inside the cell reaches its partial vapor pressure. Once equilibrium is reached between the vapor and the solid surface (source), the composition of the gas will be same as the source.

The chalcogenide base glass deposition process begins by spinning a 3 μm layer of AZ 4330 positive photoresist on the sample. AZ 4330 is a thicker photoresist than OCG 825 that was used previously and this will ensure complete coverage of the channel walls and edges. A soft bake is then performed at 78 $^{\circ}\text{C}$ for 20 minutes. At this time, the solid electrolyte film pattern is formed using a dark field mask and the Karl Suss mask aligner for exposure, exposing for 58 s at 3.8 mW/cm^2 . The pattern is then developed using 1:3 diluted solution of AZ 400K developer for 1 minute and 20 seconds. After developing the pattern, a 70 nm film of $\text{Ge}_{0.30}\text{Se}_{0.70}$ is deposited followed by a 17 nm film of Ag without breaking the vacuum. The deposition is performed using an Edwards thermal

evaporator (model E306A) with a base vacuum pressure of 3×10^{-6} Torr. Afterwards, the sample is dipped in acetone for 15 minutes to lift-off the deposited films from the undeveloped areas. At this point, the solid electrolyte is completed by illuminating the sample with ultra violet light for 20 minutes at 4.4 mW/cm^2 . Any excess silver left after the photodiffusion process is removed by dipping the sample in a silver etch solution of 50 ml DI water and 7 grams of $\text{Fe}(\text{NO}_3)_3$ for 30 s. A light field optical mask is used to pattern the electrodes on the solid electrolyte region on either side of the channel. A 100 nm layer of Ag is deposited to form the electrodes, followed by acetone lift-off for 45 minutes to remove the unwanted silver. The electrodes are then covered with silver paste and heated in an oven at $110 \text{ }^\circ\text{C}$ for 15 minutes for curing purposes. A schematic of the completed testbed is shown in Figure 1 below.

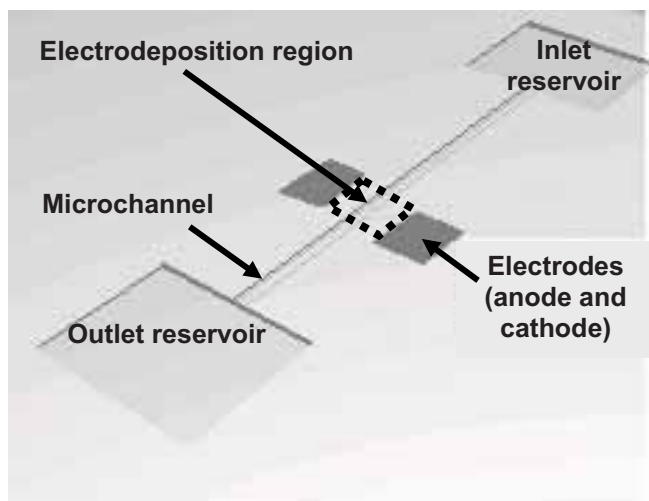


Figure 1: Schematic of microfluidic testbed showing location of micro- valve between control electrodes.

To cap the silicon microchannels, we use a polydimethyl siloxane (PDMS) layer. The PDMS is made by mixing 10 parts of Sylgard 184 Silicone elastomer and 1 part of curing agent (Dow Corning). Curing is performed in an oven at $70 \text{ }^\circ\text{C}$ for 15 minutes. Note that the reservoirs are $18 \mu\text{m}$ deep, while the microtubes which will feed the fluid into the system are $90 \mu\text{m}$ wide. Therefore, to obtain a good seal, an impression of the microtube is formed in the PDMS during the curing step.

4 RESULTS AND DISCUSSION

The test fluid used to obtain the results reported below is deionized (DI) water. This fluid is made to flow through the microchannels using a syringe pump, in which a syringe is housed in a driver actuated by a stepper motor. Unfortunately, even though this apparatus can be set up to drive flow through our testbed, it was not possible to accurately determine the pressure exerted on the fluid.

However, the lack of knowledge of the pressure was not deemed critical in this initial study as we were more interested in a comparative analysis between valve conditions. The inlet reservoir of the microchannel is connected to the syringe by a microtube. The microtube (Polymicro Technologies) is made of synthetic fused silica with an inner diameter of $20 \mu\text{m} \pm 2 \mu\text{m}$ and buffer coated with polyimide. As mentioned previously, outer diameter is $90 \mu\text{m} \pm 6 \mu\text{m}$. When covering the channel with the PDMS cap, the microtube is first placed inside the impression formed during curing and then both the cover and the tube are placed on top of the microchannel to form a tight seal. The fluid flow through the microchannels was videotaped and digitized using Media100 software.

Electrodeposition is stimulated by applying a voltage of 20V between the electrodes. Such a high voltage was required to overcome the high resistance of the electrolyte layer and drive sufficient current to grow a substantial electrodeposit in a reasonable time (a few tens of seconds). The growth rate in this case was estimated to be $8.5 \mu\text{m/sec}$. Figure 2 is an optical micrograph of a typical electrodeposit spanning the channel region. The maximum height of this deposit, determined by atomic force microscopy (AFM), is in the order of $0.6 \mu\text{m}$. Our previous work has shown that such a deposit is sufficient to significantly increase the hydrophobicity of the electrolyte surface [2].

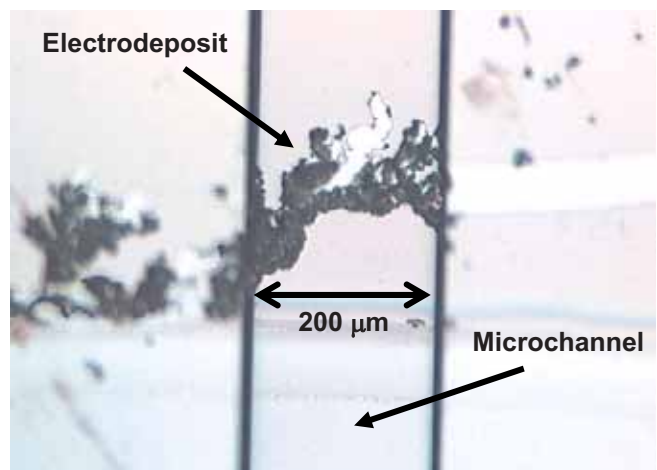


Figure 2: Optical micrograph of a silver electrodeposit that has been formed on the surface of a Ag-Ge-Se solid electrolyte in a $200 \mu\text{m}$ wide, $18 \mu\text{m}$ deep microchannel.

More revealing is the scanning electron micrograph of Figure 3. This shows how the sub- $1 \mu\text{m}$ high electrodeposits (the bright regions on the floor of the channel on the left-hand side of the micrograph) cover the channel and also how “flat” they are in relation to the total channel depth. Also visible but not quite as obvious in this image are the electrodeposits on the sloping walls of the microchannel (the flat but sloping nature of the walls is a direct consequence of the non-isotropic KOH etch used to

form the silicon channel, as discussed in the previous section). Note that the electrodeposits cover a relatively small percentage of the surface area of the electrolyte. However, as we will demonstrate in the remainder of this section, these sparse and low features are indeed able to control fluid flow in the channel.

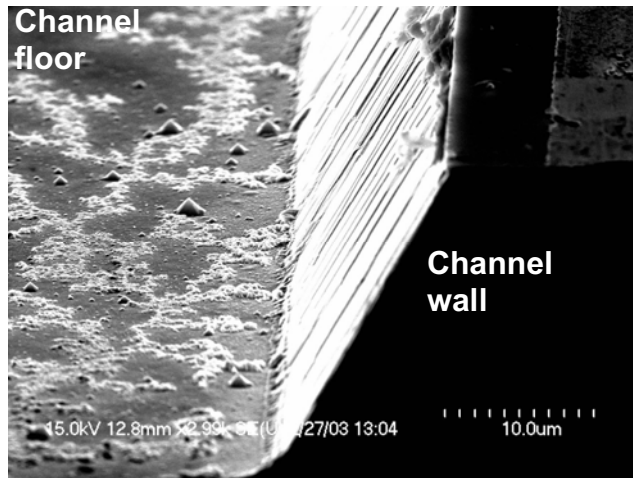


Figure 3: Scanning electron micrograph of electrodeposit on channel floor and wall. The bright features are the silver electrodeposits and the sloping wall of the channel is due to the anisotropic etch used.

Figure 4 shows two frames from one of our videos of fluid flow to illustrate the operation of the microvalve. The long narrow regions across the center of the images are the channels and edges of the inlet and outlet reservoirs are clearly visible at either end. The electrode/valve regions cover the middle third of the channels and the darker material in the channels and reservoirs is the test fluid. Figure 4(a) shows the results of fluid flow for an “open” valve (no electrodeposit has been formed), 6 seconds after the fluid enters the valve region (12 seconds total flow time in the channel). As may be seen by the position of the marker (arrow), the flow has progressed to the outlet end of the valve in this time and continues to flow, eventually filling the reservoir. Figure 4(b) is the “inhibited” valve case, in which the electrodeposit has been grown across the channel using the conditions described above. After 6 seconds of flow in the channel from the inlet, the fluid front stops abruptly at the front edge of the valve region. However, since the syringe pump was left running, the pressure continued to increase and the fluid front could be seen to move forward very slowly. This movement was not continuous and was actually quite erratic, presumably because several elongated electrodeposits had grown across the channel in the long valve region and the meniscus was “jumping” each of these as the pressure increased. The flow stalled for an extended period at the point indicated, 35 seconds after it entered the valve region (41 seconds after starting to flow in the channel). After the occurrence of additional fluid front jumps with increasing pressure, the

flow completely stopped after 71 seconds so that the fluid never reached the outlet reservoir in the case of the inhibited valve.

5 CONCLUSIONS

There are several interesting points to be taken from these initial results. The increase in contact angle and hydrophobicity created by the low profile electrodeposit is indeed sufficient to stop pressure-driven flow. We are continuing to investigate this, not only with pressure-driven flow but also with capillary flow. The fact that it takes the same amount of time for the fluid to flow from the start of the channel to the valve region for both open and inhibited valves is to be expected as there will be no build-up of air pressure ahead of the fluid flow in the case of the “closed” valve. This is because the maximum electrodeposit height is only 0.6 μm but the channel depth is 18 μm , so there is almost no additional resistance to the flow of air in the space ahead of the fluid. This is unique to this type of “surface control” valve and could lead to other applications, including separation of materials.

Clearly, much more work has to be performed before this microvalve can be implemented in working micro-analytical systems but these initial results hold great promise for the technique and demonstrate the feasibility of a potentially inexpensive and reliable microvalve that lacks mechanical moving parts.

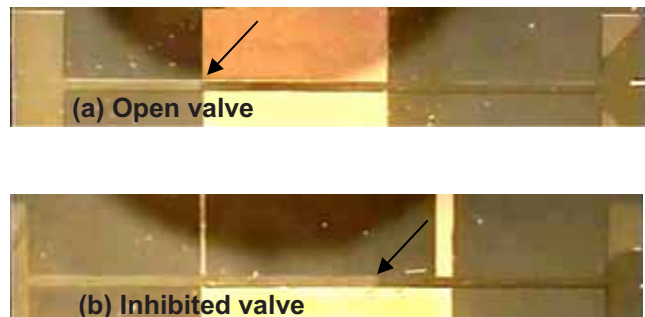


Figure 4: Demonstration of valving of pressure-driven flow in a microchannel. The arrows mark the position of the fluid front. (a) Open valve after 6 seconds of flow and (b) inhibited valve after 35 seconds of flow in the valve region (6 second delay from inlet to valve edge in both cases).

REFERENCES

- [1] D. Figeys and D. Pinto, *Analytical Chemistry*, vol. 72/9, 330 (2000).
- [2] M.N. Kozicki, P. Maroufkhani, and M. Mitkova, *Superlattices and Microstructures*, vol. 34/3-6, 467 (2004).
- [3] M.N. Kozicki, M. Mitkova, J. Zhu, and M. Park, *Microelectronic Engineering*, vol. 63, 155 (2002).
- [4] M.N. Kozicki, M. Mitkova, and J.P. Aberouette, *Physica E*, vol. 19, 161 (2003).